

DOI: 10.1002/cbic.200800153

# Modular Assembly Using Sequential Palladium Coupling Gives Easy Access to the SMOc Class of Cellular Transporters

Anne-Sophie Rebstock,<sup>[a]</sup> Cristina Visintin,<sup>[a]</sup> Elisabetta Leo,<sup>[b]</sup> Cristina Garcia Posada,<sup>[a]</sup> Sarah R. Kingsbury,<sup>[b]</sup> Gareth H. Williams,<sup>[b]</sup> Kai Stoeber,<sup>[b]</sup> and David L. Selwood<sup>\*[a]</sup>

*Dedicated to Professor Willie Motherwell on the occasion of his 60th birthday.*

The transducing ability of the third helix of transcription factor homeodomains is effectively mimicked by a biphenyl system displaying guanidine groups. The biphenyl class of small molecule carriers (SMoCs) can carry biomolecules into a wide variety of cell types. A “combinatorial” approach to the synthesis of SMOcs is described using sequential Pd<sup>0</sup> coupling chemistry to assemble the molecules from highly functionalized building blocks. SMOcs coupled to the DNA licensing repressor protein

geminin can inhibit DNA replication in vitro. We conducted a structure–activity investigation utilizing a range of SMOc–geminin conjugates and demonstrate that both electrostatic and structural features are important for efficient uptake and functional activity. The best analogue was more efficient than either (Arg)<sub>4</sub> or (Arg)<sub>8</sub> linked to geminin. Effective inhibition of DNA synthesis was achieved in fibroblasts and osteosarcoma cell lines.

## Introduction

The homeoprotein transcription factors are internalized by and secreted from cells and thus may participate in cell–cell signaling.<sup>[1]</sup> This ability to transfer between cells is mediated by the homeodomain, specifically the third helix being responsible for the internalization function with an adjacent sequence being responsible for the secretion (Figure 1). The 16-amino-acid peptide sequence (termed penetratin) derived from the third helix is an efficient cell-penetrating peptide (CPP) and has been used to carry a wide variety of biomolecules into cells. A basic peptide from the HIV-1 transcription factor tat<sup>[2]</sup> has also been used as a CPP and many other peptide CPP variants have been reported.<sup>[3,4]</sup>

In general, CPPs are not more than 30–35 amino acids<sup>[5–8]</sup> in length. CPPs are able to transport a diverse range of molecules, for example peptides, proteins and DNA, into cells.<sup>[9,10]</sup> Although the bulk of the work on CPPs was carried out in vitro, some notable successes have been achieved in vivo<sup>[9]</sup> including a remarkable rescue of purine nucleoside-deficient mice with exogenously delivered protein.<sup>[10]</sup> We recently reported on a small-molecule mimic of the third helix of a homeodomain employing a biphenyl system as a rigid chemical scaffold to display amino-acid side-chain functionality.<sup>[11]</sup> Use of polyphenyl systems to mimic  $\alpha$ -helices has been reported by Hamilton<sup>[12]</sup> and also Jacoby.<sup>[13]</sup> The rigidity of this chemical scaffold is central to this approach as it allows mimicry of the helical region in a compact molecular unit. In contrast, small molecules are random coils in solution and may only show secondary structure in special solvents.<sup>[14,15]</sup> These small-molecule carriers (Figure 1), which we termed SMOcs, efficiently deliver dye molecules and proteins into multiple cell types. The


SMOcs have a low molecular weight (compared with CPPs), are easy to conjugate to the cargo, and as reported here, straightforward to synthesize. Other groups have synthesized small molecules containing guanidines, that are able to transport cargoes inside cells but these are not conformationally constrained.<sup>[16,17]</sup>

In order to conduct a wider range of biological studies, we required access to analogues and larger quantities of SMOcs. However, the previously reported synthesis for SMOcs<sup>[11]</sup> was linear, laborious and not suitable for large-scale preparations. We report here an improved “combinatorial” convergent synthesis allowing rapid assembly of analogues based on a biphenyl scaffold. This new route allowed the synthesis of a range of SMOc analogues, enabling the first meaningful structure–function study of these compounds. For simplicity, we use the terminology 2G, 3G, and 4G to indicate a SMOc derivative with two, three or four guanidine groups.

[a] Dr. A.-S. Rebstock,<sup>+</sup> Dr. C. Visintin,<sup>+</sup> C. Garcia Posada, Dr. D. L. Selwood  
Biological and Medicinal Chemistry Group,  
Wolfson Institute for Biomedical Research, University College London  
Gower Street, London, WC1E 6BT (UK)  
E-mail: d.selwood@ucl.ac.uk

[b] Dr. E. Leo,<sup>+</sup> Dr. S. R. Kingsbury, Prof. G. H. Williams, Dr. K. Stoeber  
Cancer Research UK Chromosomal Replication Group,  
Wolfson Institute for Biomedical Research, University College London  
Gower Street, London, WC1E 6BT (UK)

[\*] These authors contributed equally to this work.

 Supporting information for this article is available on the WWW under <http://www.chembiochem.org> or from the author.

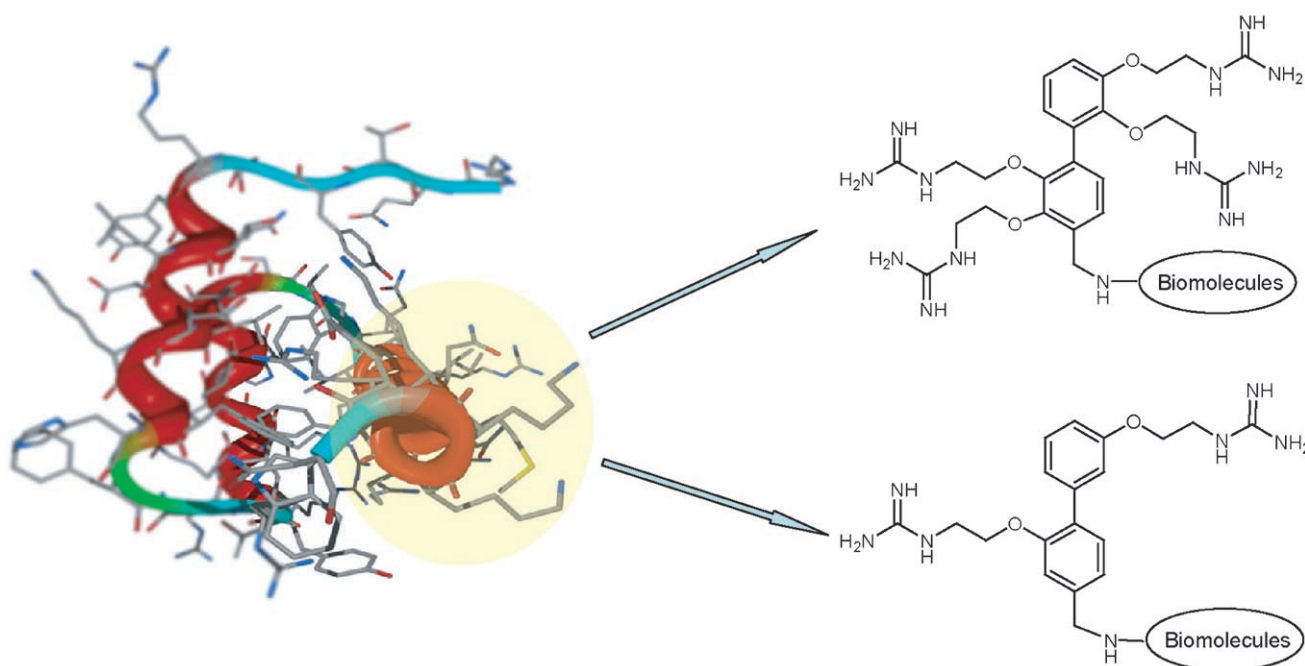


**Figure 1.** The antennapedia homeodomain showing the third helix (highlighted) utilized in the design of 4G-SMoC (top) and 2G-SMoC (bottom).

## Results

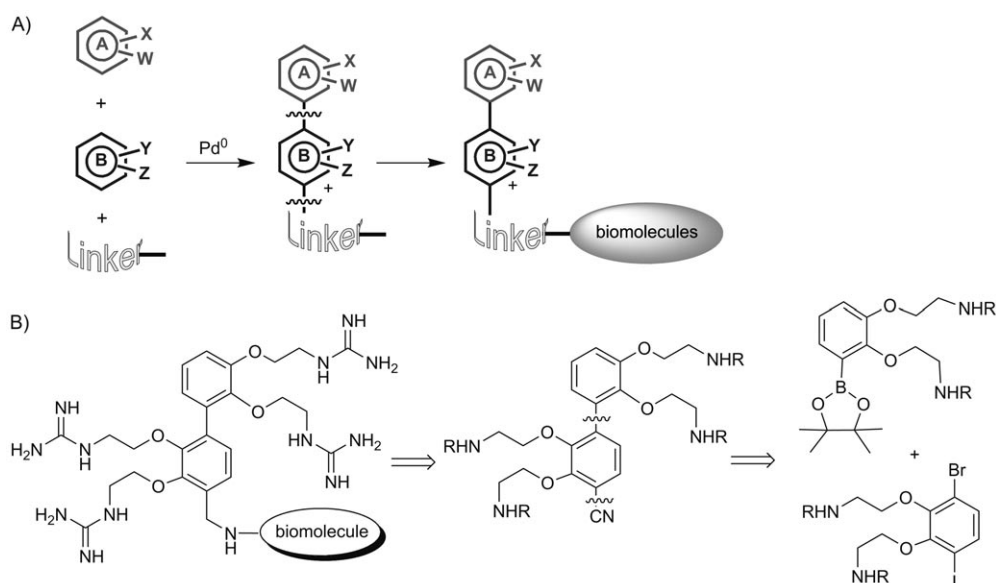
### Synthetic design

In principle, simple assembly of appropriately decorated benzenes would allow access to a wide range of substituted SMOCs (Scheme 1A). Recent developments in Pd<sup>0</sup> coupling chemistry allow the retrosynthetic analysis shown. The new convergent synthetic methodology is illustrated for 4G-SMoC (Scheme 1B) and is dependent on the Suzuki–Miyaura<sup>[18]</sup> Pd<sup>0</sup> coupling of fully alkylated polyphenols. This key step in the synthesis allowed us to avoid the early yield-limiting step of tetra-alkylation present in the previous reported method. We

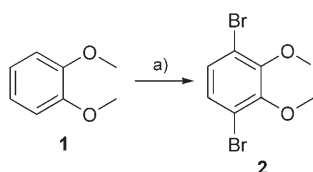
could synthesize a range of analogues through combinatorial assembly of different building blocks. We chose to generate the amino linker function late in the synthesis through simple reduction of a cyano group, avoiding tedious protection–deprotection protocols. Again, we utilize Pd<sup>0</sup> chemistry to directly couple the cyano group to a halobenzene allowing building block assembly of biphenyl and linker.

### A key 1,4-dihalobenzene intermediate

We first prepared the dibromodimethoxybenzene<sup>[19]</sup> **2** (Scheme 2) by bismetalation of veratrole and subsequent trap-

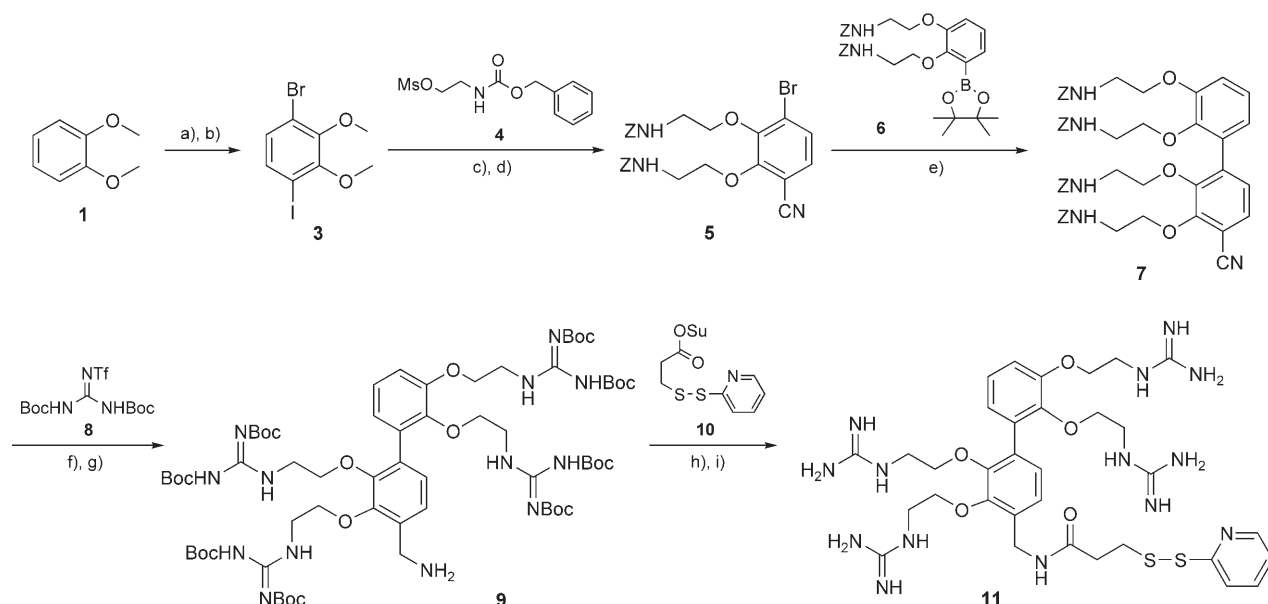


**Scheme 1.** A) Synthetic design showing the combinatorial assembly of SMOC and linker groups, and B) detailed retrosynthesis of 4G-SMoC.



**Scheme 2.** Synthesis of dibromocatechol **2**. Reagents: a) BuLi, TMEDA, 2 h, room temperature, then Br<sub>2</sub>, -78 °C then warm to room temperature (16%).

ping by C<sub>2</sub>Br<sub>2</sub>Cl<sub>4</sub>, but obtained a low yield (16%). In addition, there was no discrimination between the two halogens possible for the subsequent Pd<sup>0</sup> cross couplings. To overcome this problem we decided to synthesize compound **3** (Scheme 3) which contains two different halogens. The intermediate silyl compound was obtained by one pot, sequential *ortho* metallations with TMSCl and C<sub>2</sub>Br<sub>2</sub>Cl<sub>4</sub> quenches.<sup>[20,21]</sup> Trapping the monolithiated veratrole before the second metallation was much more efficient than utilizing the dilithio intermediate. The bromotrimethylsilyl intermediate was then treated with iodine monochloride in DCM to afford the iodobromo derivative **3**. After cleavage of the methoxy groups with boron tribromide, the bis-alkylation of the bromiodocatechol with the mesylate **4** proceeded in good yield (59%). In the first instance, we used *tert*-butoxycarbonyl (Boc) as the protecting group. Unfortunately, this was found to be unstable during the long reaction time required to complete the bis-alkylation. Therefore, we switched to the more stable benzyloxycarbonyl (Z) protection.



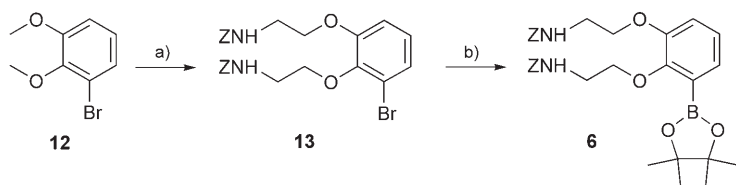
**Scheme 3.** Synthesis of 4G-SMoC **11** Reagents: a) BuLi, TMEDA, Et<sub>2</sub>O, 1 h, room temperature, then TMSCl, 16 h, room temperature; then BuLi, TMEDA, 2 h, room temperature; then C<sub>2</sub>Br<sub>2</sub>Cl<sub>4</sub>, 1 h, -40 °C; then warm to room temperature (89%); b) ICl, DCM, 2 h, -40 °C (26%); c) BBr<sub>3</sub>, DCM, 16 h, room temperature; then **4**, DMF, Na<sub>2</sub>CO<sub>3</sub>, 24 h, 80 °C (59%); d) Zn(CN)<sub>2</sub>, Pd<sub>2</sub>dba<sub>3</sub>, dpfp, Zn(OAc)<sub>2</sub>, Zn, DMA, 140 °C, 10 min, MW (61%); e) **6**, PdCl<sub>2</sub>dppf, K<sub>3</sub>PO<sub>4</sub>, toluene, water, 18 h, 100 °C (100%); f) HBr, DCM, 90 min, room temperature; then **8**, Et<sub>3</sub>N, DCM, 16 h, room temperature (65%); g) Raney-Ni, NH<sub>4</sub>OH, THF, H<sub>2</sub>, 16 h (44%); h) **10**, DIEA, DCM, 16 h, room temperature (11%); i) TFA/H<sub>2</sub>O/TIPS (95:2.5:2.5), 3 h, room temperature (100%).

### Sequential Pd<sup>0</sup> coupling allows the synthesis of 4G-SMoC

The Cbz-protected iodobromo compound was engaged in a microwave-promoted palladium-catalyzed monocyanoation.<sup>[22]</sup> This reaction was completed in 10 min at 140 °C in DMA, with Pd<sub>2</sub>dba<sub>3</sub>/dppf as the catalyst and Zn(CN)<sub>2</sub> as the cyanide source producing the bromocyano derivative **5** in good yield (61%; Scheme 3, step d). The quantity of zinc cyanide was crucial since the use of more than 0.5 equivalents resulted in the formation of the dicyano compound. The Suzuki–Miyaura coupling of **5** with the boronic ester **6** produced the polyalkylated biphenol **7** in excellent yield (100%). The order in which these two reactions were undertaken was critical. In fact, when we attempted to do the coupling prior to the cyanation step, a mixture of the desired product, bis-cross-coupling product and deiodinated compound was obtained. The purification of this mixture proved difficult, and the overall yield was much lower (24–35% depending on the coupling conditions).

After deprotection of the Z groups with hydrogen bromide, the resulting tetra-amino compound was guanidilated. Of the guanidilating reagents<sup>[23]</sup> tested, only *N,N*-di-Boc-*N'*-trifluoromethanesulfonyl-guanidine (**8**)<sup>[24]</sup> permitted the reaction to go to completion. The intermediate tetra-amine had to be carefully dried before reacting with **8**; otherwise incomplete conversion occurred. Reduction of the cyano moiety was performed under atmospheric pressure of hydrogen, with Raney-Nickel as a catalyst in the presence of ammonia.<sup>[25]</sup> The benzylamine intermediate **9** was coupled to SPDP **10** under standard activated-ester conditions. Deprotection of the Boc-protected compounds using a mixture of TFA/H<sub>2</sub>O/triisopropylsilane (95:2.5:2.5), gave the tetraguanidine **11** ready for coupling to a protein Cys-SH.

The boronic ester **6** is the key intermediate in the synthesis of different SMOc analogues. It was synthesized starting from bromoveratrole **12** (Scheme 4). This compound, prepared according to a known procedure,<sup>[26]</sup> was treated with boron tribromide and the resulting catechol alkylated with **4** to provide



**Scheme 4.** Synthesis of boronic ester **6**. Reagents: a)  $BBr_3$ , DCM, 16 h, room temperature; then **4**, DMF,  $CS_2CO_3$ , 2 h,  $100^\circ C$  (45%); b) bispinacolatodiborane,  $PdCl_2dppf$ , KOAc, DMSO,  $80^\circ C$ , 72 h (30%).

**13**. Cesium carbonate was used instead of sodium carbonate (used for the synthesis of **5**). This speeded up considerably the bis-alkylation reaction, which was performed in 2 h instead of the 16 h required previously. Compound **13** was then engaged in a palladium-catalyzed borylation<sup>[27]</sup> to afford **6**. With a flexible modular synthesis now in place, we applied this methodology to the synthesis of a range of different SMOc analogues.

#### Changing the order of the Pd<sup>0</sup> couplings gives different substitution patterns

To explore the influence of the position of the guanidine side chains, we prepared compounds **18**, **20**, **23**, and **26**. These bis-guanidylated biphenyl analogues were synthesized from the same starting material, namely the commercially available bromiodoanisole **14** (Scheme 5). Cleavage of the methoxy group followed by the alkylation of the resulting phenol afforded **15** in good yield (60%). An advantage of this methodology is that, according to the order of the synthetic transformation, mono-cyanation or mono-Suzuki coupling, we could obtain four different analogues. Mono-cyanation, performed under the same conditions as for 4G-SMOc, afforded **16** in good yield (75%). In this case, we were able to use commercially available 2- and 3-hydroxyphenylboronic acids. Thus, Suzuki cross coupling and subsequent alkylation of the phenol intermediates enabled us to prepare **17** (54%) and **19** (62%), respectively. After introducing the Boc-protected guanidines, the cyano groups were reduced affording free amines which were coupled with the disulfide linker. Final deprotection of the guanidines produced **18** and **20**. On the other hand, mono-Suzuki couplings performed on **15** using the two previously described hydroxyphenylboronic acids afforded the corresponding phenols, which were then alkylated to give **21** (54%) and **24** (52%). These substrates were engaged in the cyanation reaction. In this case, the temperature could be raised to  $160^\circ C$ , since there was no risk of dicyanation, and **22** (76%) and **25** (84%) were therefore obtained in better yield. The final compounds **23** and **26** were prepared using the same protocol (Scheme 3). Unfortunately, the hydrogenation conditions used previously did not give the desired amino intermediate in sat-

isfactory yield (<20%). To increase this yield, we investigated several reduction conditions. The best result was obtained with a mixed catalyst  $Pd^0$ -Raney nickel under hydrogen pressure.<sup>[28]</sup> The yield-limiting step was coupling of the amino group with the linker. This is probably due to the partial decomposition of the sensitive disulfide bond during purification. Further development of linker technology is underway in our laboratory.

#### Analogues exploring other structural features

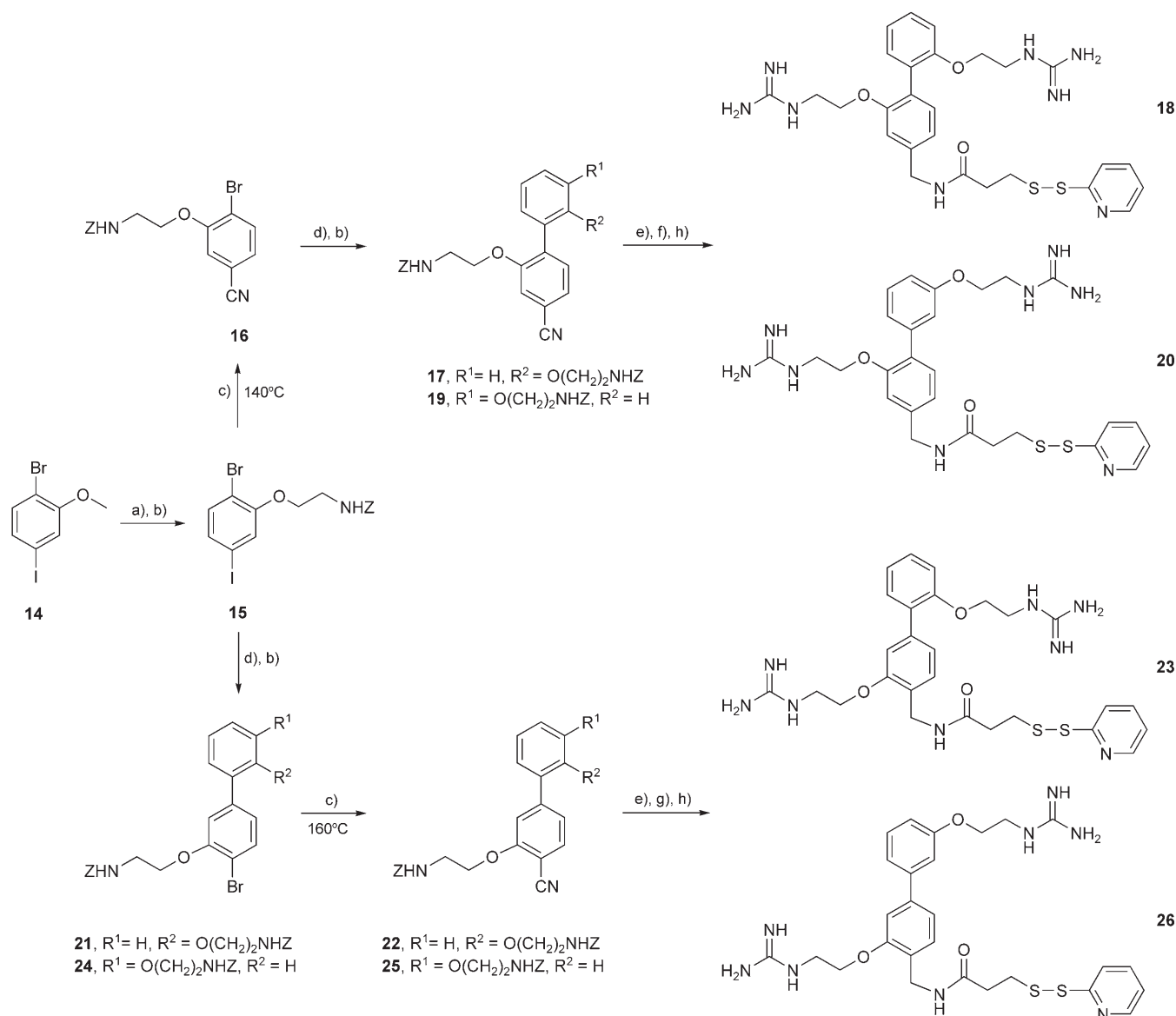
**Mono-phenyl analogue:** We synthesized the mono-phenyl analogue **28** (Scheme 6) in order to evaluate its efficiency to deliver a cargo in comparison with the biphenyl analogues. This would allow us to assess the contribution of the biphenyl structure. Cyanation and subsequent guanidylation of **13** provided **27**. This compound was coupled to the linker after reduction to the amino group by hydrogenation. Deprotection of the guanidines afforded the 2G-mono-phenyl-SMOc **28**.

**Linker position:** To investigate the influence of the position of the linker, we synthesized **31** and **33** starting from the commercially available bromocyanophenol **29** (Scheme 7). This compound already contains the cyano moiety allowing us to shorten considerably the synthesis. Compound **29** was alkylated by using the cesium carbonate procedure (68%). The resulting alkylated compound was then engaged in a Suzuki cross-coupling reaction with 2- or 3-hydroxyphenylboronic acids, providing **30** (80%) and **32** (95%), respectively, after alkylation of the intermediate phenols. The guanidines and the linker were then introduced as previously described yielding **31** and **33** after final deprotection.

**Increasing number of guanidine substituents:** In order to evaluate the influence of the number of guanidine groups we also considered that it would be interesting to synthesize the 3G-SMOc analogue **35** (Scheme 7). Alkylation of **29** and coupling of the resulting compound with boronic ester **6** afforded **34** in excellent yield (93%). The 3G-SMOc **35** was then obtained using the same procedure as before. The synthesis of this compound was shorter and more efficient than that of the other SMOc analogues, making it a good candidate for future study.

#### The biphenyl group is necessary for significant cellular uptake

To determine the ability of SMOcs to carry biomolecules into cells, we utilized live confocal microscopy and fluorescence activated cell sorting (FACS) analysis. SMOcs were coupled with the nuclear protein geminin,<sup>[29]</sup> a repressor of origin licensing, through a disulfide bond. For these studies geminin was labeled with the dye Alexa Fluor 488 (**g\***). Live confocal microscopy images for four representative SMOc-geminin-Alexa Fluor analogues, **11-g\***, **28-g\***, **33-g\***, and **35-g\*** are shown (Figures 2A–D and Figure S1 in the Supporting Information). Cellular uptake was studied in two cell lines, WI-38 human diploid fibroblasts (HDF) and human osteosarcoma cells (U2OS). When U2OS cells were treated with the fluorescent tagged

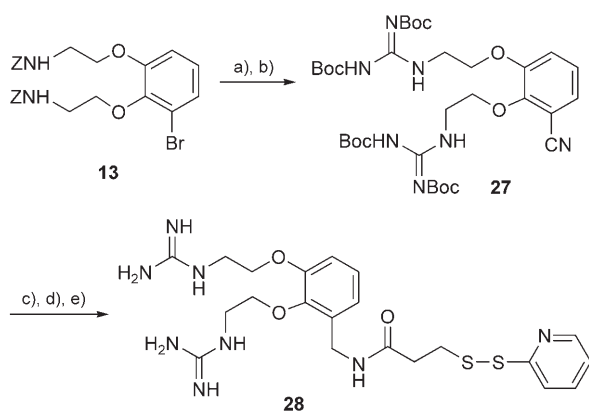


**Scheme 5.** Synthesis of 2G-SMoCs, compounds **18**, **20**, **23**, and **26**. Reagents: a)  $\text{BBr}_3$ , DCM, 16 h, room temperature; b) **4**, DMF,  $\text{Cs}_2\text{CO}_3$ , 4 h,  $80^\circ\text{C}$  (60%); c)  $\text{Zn}(\text{CN})_2$ ,  $\text{Pd}_2\text{dba}_3$ , dppf,  $\text{Zn}(\text{OAc})_2$ , Zn, DMA, 10 min, MW; d) 2- or 3-hydroxyphenylboronic acid,  $\text{PdCl}_2\text{dppf}$ ,  $\text{K}_3\text{PO}_4$ , toluene, water, 18 h,  $100^\circ\text{C}$ ; e) HBr, DCM, 90 min, room temperature; then **8**,  $\text{Et}_3\text{N}$ , DCM, 16 h, room temperature; f) Raney-Ni,  $\text{NH}_4\text{OH}$ , THF,  $\text{H}_2$ , 16 h; then **10**, DIEA, DCM, 16 h, room temperature; g) Raney-Ni, Pd/C,  $\text{NH}_4\text{OH}$ , dioxane, water,  $\text{H}_2$  (5 atm), 16 h; then **10**, DIEA, DCM, 16 h, room temperature; h)  $\text{HCO}_2\text{H}$ , 2 h,  $50^\circ\text{C}$ .

proteins, the highest uptake was detected when the cells were incubated with the 4G-SMoC-protein **11-g\*** (Figure 2D) and the lowest when treated with the 2G-SMoC-protein **28-g\***. In the case of WI-38 HDF, the difference in uptake was not obvious by this method, but a preferential perinuclear and nuclear localization was observed when geminin was linked to compounds **35-g\*** and **11-g\*** containing three and four guanidines, respectively (Figure S1). These data suggested a role for electrostatic forces in the efficiency of the delivery and cargo localization. In both cell lines, poor uptake was detected when the cells were incubated with the mono-phenyl compound **28-g\*** and this compound was not used in further studies.

### Flow cytometry shows that SMoC-geminin conjugates enter cells

Live microscopy provided qualitative information on the sub-cellular localization and uptake efficiency of internalized SMoC-geminin conjugates. We turned to FACS analysis to assess the relative amounts of cellular uptake and the percentage of cells internalizing SMoC-geminin. Cell populations were analyzed by FACS after treatment with different SMoC analogues conjugated to geminin labeled with Alexa Fluor 488. The percentage of fluorescent cells obtained from this experiment were analyzed for both cell lines (Figure 3, gray bars). Cells treated with labeled geminin conjugated to SMoC show a clear shift in the FACS profile towards higher fluorescence



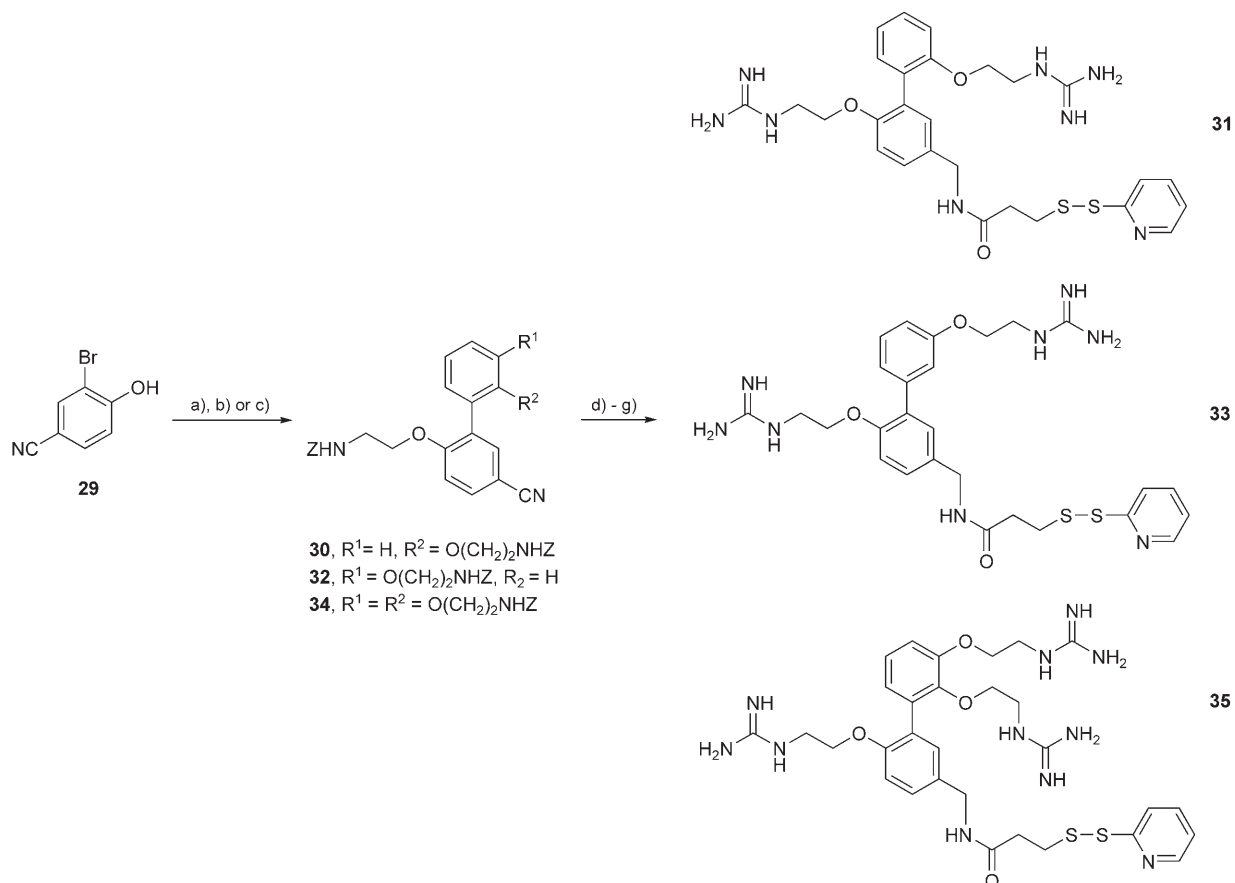
**Scheme 6.** Single phenyl unit bis-guanidine compound **28**. Reagents: a)  $\text{Zn}(\text{CN})_2$ ,  $\text{Pd}_2\text{dba}_3$ ,  $\text{dppf}$ ,  $\text{Zn}(\text{OAc})_2$ ,  $\text{Zn}$ ,  $\text{DMA}$ ,  $160^\circ\text{C}$ , 10 min, MW (72%); b)  $\text{HBr}$ ,  $\text{DCM}$ , 90 min, room temperature; then **8**,  $\text{Et}_3\text{N}$ ,  $\text{DCM}$ , 16 h, room temperature (45%); c)  $\text{Raney-Ni}$ ,  $\text{NH}_4\text{OH}$ ,  $\text{THF}$ ,  $\text{H}_2$ , 16 h (28%); d) **10**,  $\text{DIEA}$ ,  $\text{DCM}$ , 16 h, room temperature (20%); e)  $\text{TFA}/\text{H}_2\text{O}/\text{TIPS}$  (95:2.5:2.5), 3 h, room temperature (100%).

values compared to the controls; this reveals that all SMOc-conjugated proteins can enter into the cells. Approximately 100% of U2OS cells show uptake of SMOcs while for WI-38 cells the value is between 75 and 90% (Figure 3, gray bars).

### Uptake efficiency is critically dependent on SMOc structure

The relative efficiency of uptake was assessed by comparing the intensity of the fluorescence values for the different SMOcs in the two cell lines WI-38 and U2OS.

The first six bars of the chart shown (Figure 3, colored bars) represent the uptake obtained by using the bis-guanidines (**18**, **20**, **23**, **26**, **31**, and **33**) as carrier, the seventh and eighth bars represent the data for the tris-guanidine compound **35** and the tetra-guanidine compound **11**, respectively. It is clear that the SMOcs bearing three or four guanidines are more efficient carriers than those with two guanidines. Closer inspection of the relative fluorescence data for the bis-guanidines reveals some subtle differences. The compounds **18**, **31** and **20**, **33** display the guanidine side chains in the same orientation, however, the linker is in a different position. The efficiency was higher when the linker was *para* relative to the guanidine side chain. Moreover, when the guanidine side chain is *ortho* to the linker (compounds **23** and **26**) we observed a decrease in the ability to carry the cargo inside the cells. From these data we conclude that the position of the linker is influential in determining the efficiency of the molecule. Steric hindrance by the cargo might obstruct the interaction of the carrier with the cell membrane during the uptake. An alternative explanation would be that the linker or cargo disrupts the spatial arrange-



**Scheme 7.** Synthesis of 2G-SMOcs **31** and **33** and 3G-SMOc **35** with linker in *meta* position to the phenyl ring. Reagents: a) **4**,  $\text{DMF}$ ,  $\text{Na}_2\text{CO}_3$ , 15 h,  $80^\circ\text{C}$ ; b) 2- or 3-hydroxyphenylboronic acid,  $\text{PdCl}_2\text{dppf}$ ,  $\text{K}_3\text{PO}_4$ , toluene, water, 18 h,  $100^\circ\text{C}$ ; then **4**,  $\text{DMF}$ ,  $\text{Cs}_2\text{CO}_3$ , 4 h,  $80^\circ\text{C}$ ; c) **6**,  $\text{PdCl}_2\text{dppf}$ ,  $\text{K}_3\text{PO}_4$ , toluene, water, 18 h,  $100^\circ\text{C}$ ; d)  $\text{HBr}$ ,  $\text{DCM}$ , 1.5 h, room temperature; then **8**,  $\text{Et}_3\text{N}$ ,  $\text{DCM}$ , 16 h, room temperature; e)  $\text{Raney-Ni}$ ,  $\text{NH}_4\text{OH}$ ,  $\text{THF}$ ,  $\text{H}_2$ , 16 h; f) **10**,  $\text{DIEA}$ ,  $\text{DCM}$ , 16 h, room temperature; g)  $\text{TFA}/\text{H}_2\text{O}/\text{TIPS}$  (95:2.5:2.5), 3 h, room temperature.

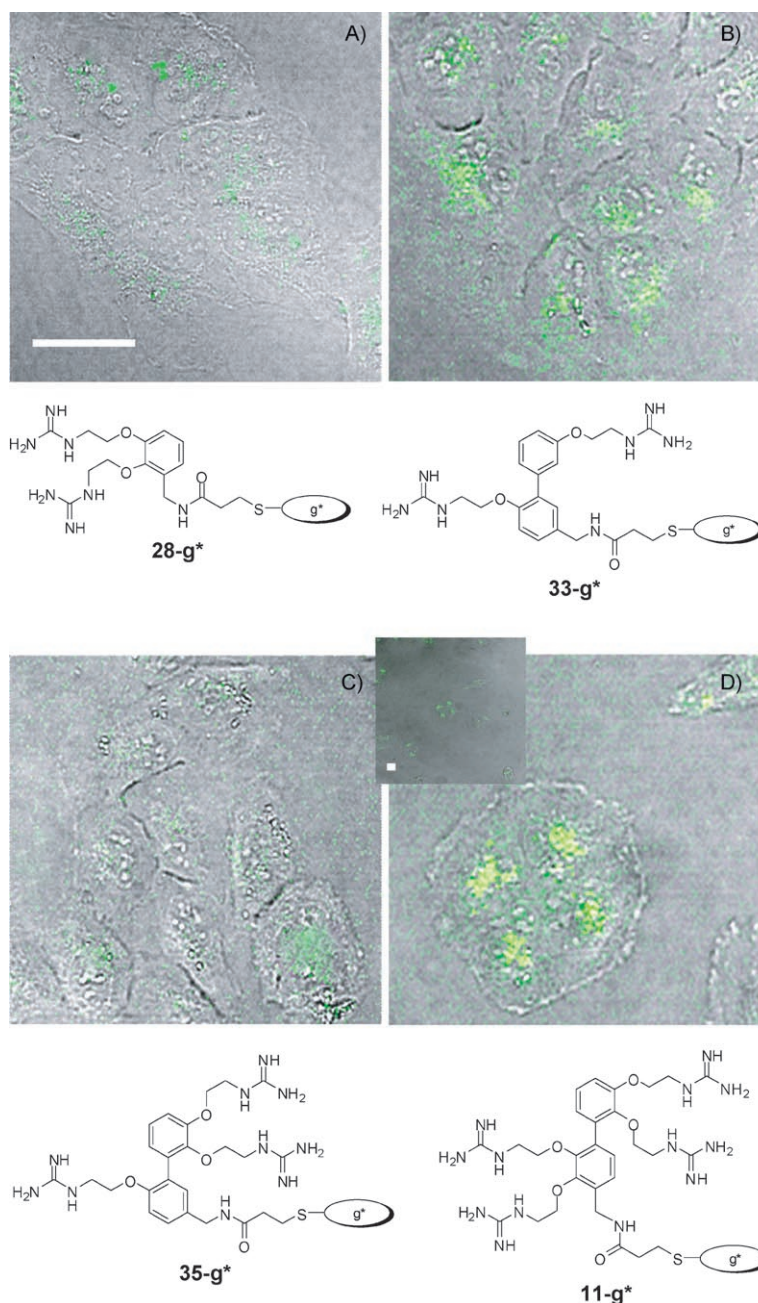


**Figure 2.** Live microscopy visualisation of delivery of SMOc analogues coupled to geminin labelled with Alexa Fluor 488 in human U2OS osteosarcoma cells. Final concentrations of geminin 10  $\mu\text{M}$ . Scale bars are 10  $\mu\text{m}$ .

ment of the guanidines preventing optimal binding to the cell. The similar efficiency of compounds **18**, **20**, **23**, and **26** indicate that the position of the guanidines on the aromatic ring does not have a significant influence on the ability to deliver cargo. In the bis-guanidines compounds **31** and **33** exhibit greater than 50% relative uptake.

To assess the ability of different SMOcs to deliver a functional protein, we treated WI-38 HDF and U2OS cells with these carriers coupled with geminin (termed **X-g**). Geminin is a 23.5 kDa protein that blocks DNA replication. For this application we used a N-terminal-truncated form of geminin ( $\Delta\text{Ng}$ ) which is not degraded during the cell cycle.<sup>[11]</sup> We then studied how cellular replication was affected by measuring the incorporation of BrdU (Figure 5). The 2G-SMOc-geminin **33- $\Delta\text{Ng}$**  and 3G-SMOc-geminin **35- $\Delta\text{Ng}$**  showed significant inhibition of

### Comparison of 4G-SMOc-geminin 11-g\* with (Arg)<sub>4</sub>-SS-geminin and (Arg)<sub>8</sub>-SS-geminin

In order to compare the efficiencies of our SMOc transporters with arginine containing peptides,<sup>[16]</sup> (Arg)<sub>4</sub>Cys-Alexa Fluor 488-geminin and (Arg)<sub>8</sub>Cys-Alexa Fluor 488-geminin were prepared by standard peptide synthesis and coupling of (Arg)<sub>n</sub>Cys-SSPy to Alexa Fluor 488-labelled geminin exactly as for 4G-SMOc. However, we found that the (Arg)<sub>n</sub> Alexa Fluor 488-geminin conjugates were significantly more adherent to the purification columns than the 4G-SMOc-Alexa Fluor 488-geminin conjugates. For this reason extensive purification of the (Arg)<sub>n</sub> conjugates was avoided and they were compared with 4G-SMOc-Alexa Fluor 488-geminin prepared in an identical fashion. The FACS data for the uptake of 4G-SMOc-Alexa Fluor 488-geminin 11-g\* compared to (Arg)<sub>4</sub>Cys-geminin and (Arg)<sub>8</sub>Cys-geminin is shown in Figure 4. All the conjugates allow some degree of cellular uptake, perhaps surprisingly both the Arg-containing peptides appear to be quite similar in their ability to internalize the Alexa Fluor 488-geminin conjugate. In contrast 4G-SMOc-Alexa Fluor 488-geminin 11-g\* is taken up by a higher proportion of cells and with greater relative fluorescence.

### Inhibition of DNA synthesis correlates with the cellular uptake efficiency

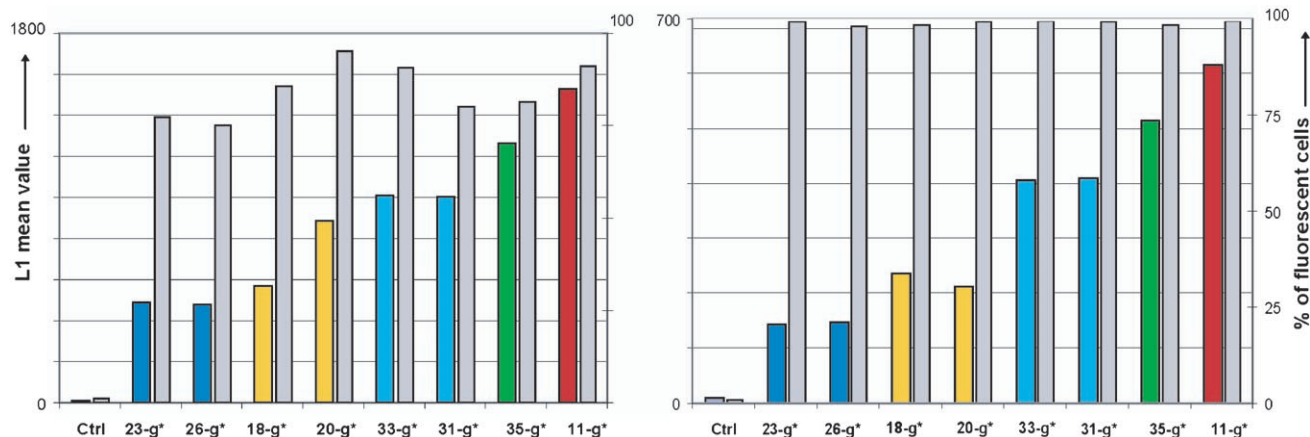


**Figure 3.** FACS analysis histogram of FACS profile of live WI-38 and U2OS cells treated by SMOc analogues coupled with labeled geminin–Alexa Fluor 488 ( $g^*$ ). The color bars represent the mean fluorescence and the gray bars the percentage of labeled cells. Final concentrations of geminin  $10 \mu\text{M}$ .

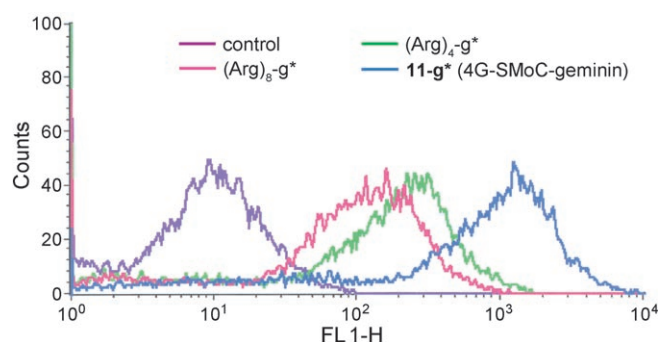


**Figure 4.** FACS analysis of WI-38 treated with  $10 \mu\text{M}$   $(\text{Arg})_4\text{-}g^*$ ,  $(\text{Arg})_8\text{-}g^*$  and  $11\text{-}g^*$ .

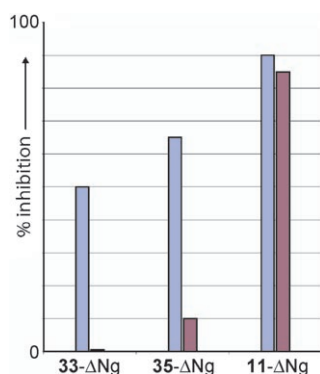


**Figure 5.** Evaluation of the inhibition of cell replication of live WI-38 (blue) and U2OS cells (purple) treated by SMOc analogues coupled with  $\Delta\text{N}$ -geminin ( $\Delta\text{N-g}$ ). Final concentrations of  $\Delta\text{N}$ -geminin  $10 \mu\text{M}$ .

DNA synthesis only for the WI-38 cell line. In contrast, 4G-SMOc–geminin  $11\text{-}\Delta\text{Ng}$  was able to inhibit at least 85% of the DNA replication in both cell lines.

## Discussion

We prepared SMOc analogues using a “combinatorial”, modular synthetic approach employing sequential  $\text{Pd}^0$  couplings as

key steps for the synthesis of SMOc analogues. In particular the versatile Suzuki–Miyaura<sup>[18]</sup> coupling reaction allowed the assembly of highly functionalized building blocks into a range of late-stage intermediates suitable for further manipulation into the SMOc–protein reactive reagents. By changing the identity of the building block it is now possible to synthesize a large range of SMOc molecules using this chemistry. Coupling the SMOc reagents to the geminin protein enabled us to identify some of the molecular features required for an efficient transporter. A clear influence of electrostatic forces was indicated as an increase in the number of guanidines led to increased uptake and improved functional activity. The biphenyl structure is necessary but the positioning of the guanidine side chains on this structure does not appear to be critical, albeit that the highly flexible side chains employed here may not adequately address this question. Is there an absolute requirement for a helical display arrangement? Clearly not as many unstructured small peptides have activity, though our molecules can mimic a helix (as in antennapedia homeodomain, for example). Does, however, the rigid “scaffold” confer better activity and are our compounds more efficient per kD as transporters as a result? We have provided additional comparison data here to suggest that they are more efficient than the simple  $(\text{Arg})_4$  and  $(\text{Arg})_8$  peptides. Our small molecules have other properties (such as increased lipophilicity) which may contribute to the transduction effect. The positioning of the linker–cargo relative to the guanidine side chain influenced activity. Steric hindrance of the cargo might interfere with the binding of the guanidines to the negatively charged phospholipids/glycolproteins on the cell surface. A more subtle effect on the conformation of the displayed guanidines cannot be discounted at this stage. Although there was no reason to assume that delivery of functional protein would correlate with our FACS and microscopy data we found similar results. We also observed that there was a greater uptake in the WI-38 cell line than in the U2OS, probably accounting for the requirement for the most efficient transporter (4G-SMOc) to enable inhibition of DNA synthesis in the osteosarcoma cells.



It is instructive to compare our molecules with those of the other nonpeptidic transporters: only the glycoside based transporters of Tor<sup>[30]</sup> have any degree of structural rigidity. Peptoid-based<sup>[16]</sup> or guanidine peptide nucleic acids<sup>[31]</sup> do not, neither do the sorbitol-based transporters,<sup>[17]</sup> which unusually confer mitochondrial subcellular localization. If we contrast these agents with our SMOCs then we can see that the biphenyl is a rigid scaffold system with increased lipophilic character. Further studies will be required to elucidate the relative contribution of spatial orientation of side chains and lipophilicity. The data presented here allow access to a wide range of SMOc structures and contributes to the optimization of SMOcs for the delivery of protein cargoes.

## Experimental Section

**Protein expression and coupling to xG-SMOc and Alexa Fluor 488:** Geminin and  $\Delta$ Ng were expressed and purified as described.<sup>[32]</sup> We conjugated geminin with Alexa Fluor 488 using the Molecular Probes Protein Labelling kit, according to the manufacturer's protocol (Invitrogen). Coupling reactions of proteins with the different SMOcs have been described.<sup>[11]</sup> The efficiency of coupling was assessed by spectrophotometric quantification of pyridine-2-thione at 343 nm and by monitoring the release of sulfhydryl groups by using Ellman's Reagent (Pierce, Rockford, IL, USA) according to Pierce protocol 22582.

**Preparation of (Arg)<sub>n</sub>Cys-geminin conjugates:** Both (Arg)<sub>4</sub>-Cys-SSPy and (Arg)<sub>8</sub>-Cys-SSPy were prepared by standard Fmoc peptide synthesis (Peptide Protein Research, Hampshire, UK) and coupled to Alexa Fluor 488-labelled geminin as described,<sup>[11]</sup> but without the final purification step.

**Cell culture:** Human U2OS and WI-38 HDF, were cultured in DMEM supplemented with FCS (10%), penicillin (100 U mL<sup>-1</sup>) and streptomycin (0.1 mg mL<sup>-1</sup>).

**Confocal microscopy:** For detection of different xG-SMOc-geminin-Alexa Fluor 488 uptake into live cells, exponentially growing cells (WI-38 HDF and U2OS) were cultured on glass coverslips. Cells were washed in PBS and incubated with fresh medium containing xG-SMOc-geminin-Alexa Fluor 488 (10  $\mu$ M). Coverslips were washed extensively in PBS, placed in a plate containing medium without Red Phenol (Gibco) and observed by live confocal fluorescence microscopy (MP-UV, Leica Microsystems GmbH, Wetzlar, Germany) by using 40 $\times$  and 63 $\times$  water immersion objectives. In order to obtain similar fluorescence intensities, WI-38 and U2OS cells required incubation with the protein conjugate for 1 and 5 h, respectively.

**Fluorescence detection by FACS analysis:** Cells were seeded in 6-well plates and incubated with xG-SMOc-geminin-Alexa Fluor 488 (10  $\mu$ M) for 3 (WI-38 cells) or 5 h (U2OS cells). Cells were then washed extensively with PBS, trypsinized for 5–10 min, resuspended in medium, washed again in cold PBS and immediately analyzed by Flow Cytometry (FACSCalibur). A total of 10000 cells per sample were counted. The mean fluorescence intensity of xG-SMOc-geminin-Alexa Fluor488-treated cell populations was compared with untreated control cells and cells incubated with Alexa Fluor 488 or geminin-Alexa Fluor 488 only.

**Cell proliferation assay:** To assess whether  $\Delta$ N-geminin retains its ability to inhibit DNA replication in cycling cells when coupled with xG-SMOc, xG-SMOc- $\Delta$ N-geminin (10  $\mu$ M) was added to WI-38

and U2OS and replenished every 24 h, for a total 72 h treatment. 71 h after the initial treatment, cells were pulse-labelled for 1 h with BrdU (10  $\mu$ M), then fixed with paraformaldehyde (4%), and treated as described.<sup>[11]</sup> Confocal fluorescence microscopy was performed on a Leica TCS DMRE confocal microscope.

## Abbreviations

Boc = *tert*-butoxy carbonyl, CPP = cell-penetrating protein, DCM = dichloromethane, DIEA = *N,N*-diisopropylethylamine, DMA = *N,N*-dimethylacetamide, DMF = dimethylformamide, DMSO = dimethylsulfoxide, DMEM = Dulbecco's Modified Eagle Medium, dppf = 1,1'-bis(diphenylphosphanyl)ferrocene, FACS = fluorescence-activated cell sorting, Fmoc = 9-fluorenylmethoxycarbonyl, HDF = human diploid fibroblasts, MS = methanesulfonyl, MW = microwave, PBS = phosphate-buffered saline, SMOc = small-molecule carrier, Su = succinimidyl, Tf = trifluoromethanesulfonyl, TIPS = triisopropylsilane, TMEDA = *N,N,N',N'*-tetramethylethylenediamine, Z = benzyloxy carbonyl.

## Acknowledgements

We thank Mitsubishi Pharma Corporation for funding for C.V. The geminin studies were funded by Cancer Research UK Programme grant C428A6263. We also would like to thank Prof. S. Moncada for his support and helpful discussions.

**Keywords:** coupling reactions · guanidin · palladium · small-molecule carriers · synthesis

- [1] A. Prochiantz, A. Joliot, *Nat. Rev. Mol. Cell Biol.* **2003**, *4*, 814–819.
- [2] M. Benkirane, K. T. Jeang, C. Devaux, *EMBO J.* **1994**, *13*, 5559–5569.
- [3] P. M. Fischer, E. Krausz, D. P. Lane, *Bioconjugate Chem.* **2001**, *12*, 825–841.
- [4] Q. L. Lu, G. Bou-Gharios, T. A. Partridge, *Gene Ther.* **2003**, *10*, 131–142.
- [5] A. Joliot, A. Prochiantz, *Nat. Cell Biol.* **2004**, *6*, 189–196.
- [6] M. Mae, U. Langel, *Curr. Opin. Pharmacol.* **2006**, *6*, 509–514.
- [7] M. Magzoub, A. Gräslund, *Q. Rev. Biophys.* **2004**, *10*, 310–315.
- [8] J. S. Wadia, R. V. Stan, S. F. Dowdy, *Nat. Med.* **2004**, *10*, 310–315.
- [9] S. R. Schwarze, S. F. Dowdy, *Trends Pharmacol. Sci.* **2000**, *21*, 45–48.
- [10] A. Toro, E. Grunebaum, *J. Clin. Invest.* **2006**, *116*, 2717–2726.
- [11] M. Okuyama, H. Laman, S. R. Kingsbury, C. Visintin, E. Leo, K. L. Eward, K. Stoeber, C. Boshoff, G. H. Williams, D. L. Selwood, *Nat. Methods* **2007**, *4*, 153–159.
- [12] B. P. Orner, J. T. Ernst, A. D. Hamilton, *J. Am. Chem. Soc.* **2001**, *123*, 5382–5383.
- [13] E. Jacoby, *Bioorg. Med. Chem. Lett.* **2002**, *12*, 891–893.
- [14] H. J. Dyson, P. E. Wright, *Annu. Rev. Biophys. Biophys. Chem.* **1991**, *20*, 519–538.
- [15] M. Magzoub, L. E. Eriksson, A. Gräslund, *Biochim. Biophys. Acta Biomembr.* **2002**, *1563*, 53–63.
- [16] P. A. Wender, D. J. Mitchell, K. Pattabiraman, E. T. Pelkey, L. Steinman, J. B. Rothbard, *Proc. Natl. Acad. Sci. USA* **2000**, *97*, 13003–13008.
- [17] K. K. Maiti, W. S. Lee, T. Takeuchi, C. Watkins, M. Fretz, D. C. Kim, S. Futaki, A. Jones, K. T. Kim, S. K. Chung, *Angew. Chem.* **2007**, *119*, 5984–5988; *Angew. Chem. Int. Ed.* **2007**, *46*, 5880–5884.
- [18] N. Miyaura, A. Suzuki, *Chem. Rev.* **2008**, *108*, 2457–2483.
- [19] M. Albrecht, *Synthesis* **1996**, 230.
- [20] M. A. Reed, M. T. Chang, V. Snieckus, *Org. Lett.* **2004**, *6*, 2297–2300.
- [21] D. L. Selwood, K. S. Jandu, *Heterocycles* **1988**, *27*, 1191–1196.
- [22] A. Zhang, J. L. Neumeyer, *Org. Lett.* **2003**, *5*, 201–203.
- [23] A. R. Katritzky, B. V. Rogovoy, *ARKIVOC* **2005**, (iv), 49–87.
- [24] K. Feichtinger, C. Zapf, H. L. Sings, M. Goodman, *J. Org. Chem.* **1998**, *63*, 3804–3805.

- [25] C. Dahmen, J. Auernheimer, A. Meyer, A. Enderle, S. L. Goodman, H. Kessler, *Angew. Chem.* **2004**, *116*, 6818–6821; *Angew. Chem. Int. Ed.* **2004**, *43*, 6649–6652.
- [26] R. V. Stevens, G. S. Bisacchi, *J. Org. Chem.* **1982**, *47*, 2396–2399.
- [27] T. Ishiyama, M. Murata, N. Miyaura, *J. Org. Chem.* **1995**, *60*, 7508–7510.
- [28] B. Klenke, I. H. Gilbert, *J. Org. Chem.* **2001**, *66*, 2480–2483.
- [29] T. J. McGarry, M. W. Kirschner, *Cell* **1998**, *93*, 1043–1053.
- [30] N. W. Luedtke, Q. Liu, Y. Tor, *Biochemistry* **2003**, *42*, 11391–11403.
- [31] P. Zhou, M. Wang, L. Du, G. W. Fisher, A. Waggoner, D. H. Ly, *J. Am. Chem. Soc.* **2003**, *125*, 6878–6879.
- [32] A. L. Okorokov, E. V. Orlova, S. R. Kingsbury, C. Bagneris, U. Gohlke, G. H. Williams, K. Stoeber, *Nat. Struct. Mol. Biol.* **2004**, *11*, 1021–1022.

---

Received: March 10, 2008

Published online on July 4, 2008